

A Search for Dense Gas in Luminous Submillimeter Galaxies with the 100-m Green Bank Telescope

T. R. Greve¹

tgreve@submm.caltech.edu

L. J. Hainline¹

A. W. Blain¹

California Institute of Technology, Pasadena, CA 91125, USA

Ian Smail²

Institute for Computational Cosmology, University of Durham, South Road, Durham DH1 3LE, United Kingdom

R. J. Ivison³

UK ATC, Royal Observatory, Blackford Hill, Edinburgh EH9 3HJ, United Kingdom

P. P. Papadopoulos⁴

Institut für Astronomie, ETH, Zürich, 8093 Switzerland

ABSTRACT

We report deep K-band (18-27 GHz) observations with the 100-m Green Bank Telescope of HCN(1-0) line emission towards the two submillimeter-selected galaxies (SMGs) SMM J02399-0136 ($z = 2.81$) and SMM J16359+6612 ($z = 2.52$). For both sources we have obtained spectra with channel-to-channel rms noise of $\sigma \leq 0.5$ mJy, resulting in velocity-integrated line fluxes better than $\lesssim 0.1$ Jy km s⁻¹, although we do not detect either source. Such sensitive observations – aided by gravitational lensing of the sources – permit us to put upper limits of $L'_{\text{HCN}} \lesssim 2 \times 10^{10}$ K km s⁻¹ pc² on the intrinsic HCN(1-0) line luminosities of the two SMGs. The far-infrared (FIR) luminosities for all three SMGs with sensitive HCN(1-0) observations to date are found to be consistent with the tight FIR-HCN luminosity correlation observed in Galactic molecular clouds, quiescent spirals and (ultra) luminous infrared galaxies in the local Universe. Thus, the observed HCN luminosities remain in accordance with what is expected from the

universal star formation efficiency per *dense* molecular gas mass implied by the aforementioned correlation, and more sensitive observations with today’s large aperture radio telescopes hold the promise of detecting HCN(1 – 0) emission in similar objects in the distant Universe.

Subject headings: cosmology: observations — galaxies: high-redshift – galaxies: ISM – galaxies: starburst

1. Introduction

The search for molecular lines at high redshifts ($z \gtrsim 1$) offers one of the richest and most exciting avenues to follow in the study of galaxy formation and evolution (Solomon & Vanden Bout 2005). The detections of rotational transitions of CO in extremely distant quasars (Carilli et al. 2002; Walter et al. 2003), high- z radio galaxies (Papadopoulos et al. 2000; De Breuck et al. 2005) and submillimeter (submm) selected galaxies (Frayser et al. 1998, 1999; Neri et al. 2003), have established that the most luminous and extreme objects in the early Universe harbour vast amounts of molecular gas ($\sim 10^{10-11} M_{\odot}$ – Neri et al. 2003; Greve et al. 2005) and have large dynamical masses ($\sim 10^{11} M_{\odot}$ – Genzel et al. 2003; Tacconi et al. 2006). Modelling of the bulk physical conditions of the molecular gas in high- z QSOs have even been possible in cases where several CO lines have been detected (Weiß et al. 2005). The success of CO observations is primarily due to its much larger abundance compared to other species as well as its easily excitable low- J (CO $J + 1 \rightarrow J, J < 3$) rotational lines, which makes it an excellent tracer of the total amount of *diffuse* ($n(\text{H}_2) \sim 10^{2-3} \text{ cm}^{-3}$) molecular gas. However, the diffuse gas only serves as a reservoir of *potential* fuel available for star formation, and is not actively involved in forming stars.

In our own Galaxy, the sites of active star formation coincide with the dense cores of giant molecular clouds (GMCs). This dense gas phase ($n(\text{H}_2) \gtrsim 10^4 \text{ cm}^{-3}$) is best traced using molecules with high critical densities such as HCN. This basic picture also appears to hold in nearby galaxies, as suggested by HCN(1 – 0) surveys of local ($z \lesssim 0.1$) Luminous Infrared Galaxies (LIRGs – $L_{\text{IR}} \sim 10^{11} L_{\odot}$) and Ultra Luminous Infrared Galaxies (ULIRGs – $L_{\text{IR}} \sim 10^{12} L_{\odot}$), which found a remarkably tight correlation between IR luminosity and HCN line luminosity (Solomon et al. 1992; Gao & Solomon 2004a,b). Recently, this relation was shown to extend all the way down to single GMCs, thus extending over 7-8 orders of magnitude in IR luminosity (Wu et al. 2005). This was interpreted as suggesting that the true star formation efficiency (i.e. the star formation rate per unit mass of *dense* gas) is the same in these widely different systems.

Attempts have been made at extending the correlation between IR and HCN luminosity to primordial galaxies at high redshifts (Barvainis et al. 1997; Solomon et al. 2003; Isaak et al. 2004; Carilli et al. 2005), resulting in four objects detected in HCN out of 8 objects observed. So far the results have been consistent with the local correlation, however, the small number of sources precludes a statistically robust conclusion as to whether the relation also holds at high redshift. Furthermore, the majority of high- z objects observed have been extremely luminous QSOs and HzRGs dominated by Active Galactic Nuclei (AGN).

The detection of HCN(1 – 0) in the $z = 2.286$ QSO F 10214+4724 (Vanden Bout, Solomon & Maddalena 2004), which marked the first high- z detection of HCN using the Green Bank Telescope (GBT), motivated us to test the capability of the GBT to probe the dense gas in a population of high- z galaxies less extreme, i.e. less AGN-dominated than F 10214+4724, but more representative of starburst galaxies in the early Universe. The goal of our study was to observe two of the most prominent examples of submillimeter-selected galaxies (see Blain et al. 2002 for a review) – a population likely to constitute the progenitors of today’s massive spheroids, and thus fundamental to our understanding of galaxy formation and evolution.

Throughout this paper we adopt a flat cosmology, with $\Omega_m = 0.27$, $\Omega_\Lambda = 0.73$ and $H_0 = 71 \text{ km s}^{-1} \text{ Mpc}^{-1}$ (Spergel et al. 2003).

2. Sources

The two submillimeter galaxies targeted with the GBT were SMM J02399–0136 ($z = 2.808$) and SMM J16359+6612 ($z = 2.517$)¹. These two sources were chosen by virtue of 1) their gravitational lensing amplifications making them amongst the brightest submm sources known (Smail et al. 1997, 2002; Kneib et al. 2004), and 2) their strong CO line emission (Frayer et al. 1998; Genzel et al. 2003; Sheth et al. 2004; Kneib et al. 2005). Moreover, while J02399 has a moderate amplification factor ($\mu \sim 2.5$) and thus is intrinsically very luminous, the extremely large amplification factor of J16359 ($\mu \sim 22$) means that this source has about an order of magnitude smaller intrinsic luminosity. Thus, our observations could potentially explore differences in the dense gas mass fraction between massive and not so massive starburst galaxies at high redshifts.

¹hereafter we shall refer to these three sources as J02399 and J16359, respectively

3. Observations and Data Reduction

The observations were carried out between March 21st and April 5th 2005 at the 100-m Robert C. Byrd Green Bank Telescope in Green Bank, West Virginia². Due to scheduling and observability constraints, J02399 received by far the most observing time: 9.6 hrs of effective integration in each polarisation, with J16359 getting only 3.3 hrs.

At the redshifts of the two sources, the HCN(1–0) line ($\nu_{\text{rest}} = 88.631$ GHz) falls within the K-band (17.6–27.1 GHz) receiver on the GBT. The K-band receiver consists of two pairs of dual circular polarisation beams, covering the frequency ranges 17.6–22.4 GHz and 22.0–27.1 GHz, respectively. In our case, the HCN(1–0) line from both sources could be observed using only one pair of beams (22.0–27.1 GHz). At ~ 25 GHz the GBT has a beam size of $\text{FWHM} = 30''$ – much larger than the source size ($\lesssim 2''$).

The observations were made in dual-beam mode, in which one feed sees the source (**ON**) and the other sees the blank sky (**OFF**). After one such scan (which in our case lasted 2 minutes), the telescope nods so that the first feed now is **OFF** and the second feed is **ON** the source, thus ensuring that one beam is always integrating on-source (except during the nodding). As backend we used the GBT Spectrometer in its moderate-bandwidth, low-resolution submode, giving 200 MHz of total instantaneous bandwidth divided into 8192 channels each of width 24.41 kHz. At 25 GHz this corresponds to a velocity-coverage of $\simeq 2400 \text{ km s}^{-1}$ and a resolution of $\simeq 0.3 \text{ km s}^{-1}$ per channel – more than enough to encompass the entire line and resolve it spectrally. This is based on the reasonable assumption that the HCN line widths are similar to those of CO (Greve et al. 2005).

Calibration was by noise-injection, in which a noise-diode is switched on and off at a rate of 1 Hz during the integration. Thus a typical data time stream can be visualised as follows:

	Beam 1	Beam 2
Scan 1:	$\overbrace{[\text{ON}_{\text{calon}}, \text{ON}_{\text{caloff}}]}^{\text{ON}_{1,1}}$	$\overbrace{[\text{OFF}_{\text{calon}}, \text{OFF}_{\text{caloff}}]}^{\text{OFF}_{2,1}}$
Scan 2:	$\overbrace{[\text{OFF}_{\text{calon}}, \text{OFF}_{\text{caloff}}]}^{\text{OFF}_{1,2}}$	$\overbrace{[\text{ON}_{\text{calon}}, \text{ON}_{\text{caloff}}]}^{\text{ON}_{2,2}}$

²The GBT is operated by the National Radio Astronomy Observatory. The National Radio Astronomy Observatory is a facility of the National Science Foundation operated under cooperative agreement by Associated Universities, Inc.

$$\begin{array}{l} \text{Scan 3:} \quad \overbrace{[\text{ON}_{calon}, \text{ON}_{caloff}]}^{\text{ON}_{1,3}} \quad \overbrace{[\text{OFF}_{calon}, \text{OFF}_{caloff}]}^{\text{OFF}_{2,3}} \\ \cdot \\ \cdot \\ \cdot \end{array}$$

The system temperature on the blank sky is then given by:

$$T_{sys}(\nu, p) = T_{cal}(\nu, p) \frac{\text{OFF}_{caloff}}{\text{OFF}_{calon} - \text{OFF}_{caloff}} + \frac{T_{cal}(\nu, p)}{2}, \quad (1)$$

where $T_{cal}(\nu, p)$ is the calibration temperature of the noise diode and is a function of frequency (ν) and polarisation (p). Instead of $T_{cal}(\nu, p)$ we adopted the mean $T_{cal}(p)$ value across the entire bandpass. Throughout the observing run the system temperature (integrated over the entire bandwidth observed) varied between 28 K in optimal conditions to 55 K in the worst cases, depending on elevation and the water vapour content of the atmosphere. Each scan was inspected by eye in order to weed out bad or abnormal looking scans.

The data were reduced using two independent methods. The first method used the GBTIDL-routine GETNOD, which takes the OFF signal from one scan and subtracts it from the ON signal in the neighbouring scan, and vice versa. In this scheme the spectra are calibrated onto the antenna temperature scale following:

$$T_{ant,j}(\nu, p) = T_{sys}(\nu, p) \frac{\text{ON}_{i,j} - \text{OFF}_{i,j+1}}{\text{OFF}_{i,j+1}}, \quad (2)$$

where $\text{ON}_{i,j} = (\text{ON}_{calon} + \text{ON}_{caloff})/2$ and $\text{OFF}_{i,j+1} = (\text{OFF}_{calon} + \text{OFF}_{caloff})/2$, and i, j represent the beam and scan number, respectively. Thus two neighbouring scans result in two independent spectra, $T_{ant,j}(\nu, p)$ and $T_{ant,j+1}(\nu, p)$. All the difference spectra are then averaged, weighted according to their system temperature, to produce the final difference spectrum for each polarisation.

As an alternative reduction scheme, we used the method of Hainline et al. (2006) which involves constructing a baseline template for each ON signal from a best-fit linear combination of its neighbouring OFF signals. We can write this as

$$T_{ant,j+1}(\nu, p) = T'_{sys}(\nu, p) \frac{\text{ON}_{i,j+1} - \text{OFF}_{i,j+1}^{\text{templ}}}{\text{OFF}_{i,j+1}^{\text{templ}}}, \quad (3)$$

where $T'_{sys} = a \cdot T_{sys,i,j} + b \cdot T_{sys,i,j+2}$ is a combination of the system temperature of the scans that make up the baseline template: $\text{OFF}_{i,j+1}^{\text{templ}} = a \cdot \text{OFF}_{i,j} + b \cdot \text{OFF}_{i,j+2}$. The parameters a and

b are the best-fit parameters which minimises the quantity $((\text{ON}_{i,j+1} - \text{OFF}_{i,j+1}^{\text{templ}})/\text{OFF}_{i,j+1}^{\text{templ}})^2$. Again, a final spectrum for each polarisation is constructed as a weighted average of all difference spectra produced in this manner. Vanden Bout et al. (2004) proposed another way of removing problematic baselines, which involves fitting a baseline template to the time-averaged spectrum containing the line. However, from a detailed comparison between the two methods, Hainline et al. (2006) demonstrated that their scheme is just as good at removing baseline-ripples at the scales one would expect to see a galaxy emission line. As a result we did not attempt to apply the method by Vanden Bout et al. (2004).

The final spectra were corrected for atmospheric attenuation using the opacity values at 23-26 GHz for the observing dates (R. Maddalena, private communication), and converted from antenna temperature to Janskys by applying an appropriately scaled version of the GBT gain-elevation curve at 43 GHz.

4. Results & Discussion

The final HCN(1 – 0) spectra of J02399 and J16359, reduced using the two independent methods described in the previous section, are shown in Figure 1. The spectra have been smoothed to 50 km s^{-1} bins. Both methods fail to get completely rid of residual baseline wiggles in the final spectra. However, the spectra reduced with GETNOD appear to be slightly less noisy than the spectra reduced with the second reduction method. The channel-to-channel rms noise of the spectra reduced using the GETNOD routine are 0.1 and 0.3 mJy, respectively. This is somewhat higher than the theoretical noise estimates of 0.07 and 0.12 mJy, calculated for a typical system temperature $T_{\text{sys}} = 38 \text{ K}$ and integration times corresponding to the ones of J02399 and J16359, respectively. Thus, it would seem that although the noise does integrate down as $t^{-1/2}$, the residual baseline wiggles prevents us from reaching the theoretical noise limit.

No emission is detected significantly above the noise at $V_{LSR} = 0 \text{ km s}^{-1}$ (or any other V_{LSR}), which corresponds to the CO redshift and thus the expected position of the HCN(1 – 0) line. However, the sensitivity of the observations allow us to put upper limits on the HCN(1 – 0) line luminosity of these two SMGs. In doing so we use the upper line flux limits derived from the spectra produced by GETNOD, as it results in the lowest noise spectra. The $3\text{-}\sigma$ upper limits are calculated following Seaquist, Ivison & Hall (1995)

$$S_{\text{HCN}(1-0)}\Delta V \leq 3\sigma(\delta v\Delta v_{\text{fwhm}})^{1/2}, \quad (4)$$

where σ is the channel-to-channel rms noise, δv the velocity resolution and Δv_{fwhm} the line width. The spectra were binned to a velocity resolution of 50 km s^{-1} . We set the HCN(1 – 0)

line widths equal to that of the CO lines – see Greve et al. (2005). This is probably a conservative estimate since in local ULIRGs, the HCN line widths are rarely larger than those of CO (Solomon et al. 1992; Gao & Solomon 2004a). The resulting upper line flux limits are 0.08 and 0.13 Jy km s⁻¹ for J02399 and J16359, respectively. From these flux limits we derive upper limits on the apparent HCN(1 – 0) line luminosities of $L'_{\text{HCN}(1-0)} \leq 5.0 \times 10^{10}$ and $\leq 6.6 \times 10^{10}$ K km s⁻¹ pc² for J02399 and J16359, respectively. Correcting for gravitational lensing we find intrinsic line luminosities of $L'_{\text{HCN}(1-0)} \leq 2.0 \times 10^{10}$ and $\leq 0.3 \times 10^{10}$ K km s⁻¹ pc². These upper limits on the HCN line luminosity are similar to those achieved towards high-*z* QSOs using the Very Large Array (e.g. Isaak et al. 2004; Carilli et al. 2005). Table 1 lists our findings along with all high-*z* HCN observations published in the literature at the time of writing. It is seen that of 10 sources observed to date only 4 have been detected – the remainder being upper limits.

In order to determine the star formation efficiency per dense gas mass, and the dense gas fraction, as gauged by the $L_{\text{FIR}}/L'_{\text{HCN}}$ and $L'_{\text{HCN}}/L'_{\text{CO}}$ ratio, respectively (Gao & Solomon 2004a,b), we need accurate estimates of the FIR and CO(1-0) luminosities.

The FIR luminosities of SMGs are generally difficult to estimate accurately, largely due to the poor sampling of their FIR/submm/radio spectral energy distributions. Furthermore, in our case the situation is complicated by the fact that most, if not all, of the sources in Table 1 contain AGN, which may be at least partly responsible for heating the dust and thus powering the FIR emission. Unfortunately, FIR/submm data from the literature do not allow for a detailed modelling of a hot ($\gtrsim 100$ K) dust component (heated by the AGN), and we are therefore unable to correct for any AGN contamination. The one exception is the $z = 3.9$ BAL quasar, APM 08279+5255, where the separate AGN vs. starburst contributions to the FIR luminosity have been determined by Rowan-Robinson (2000) who find an apparent FIR luminosity of $L_{\text{FIR}} \simeq 1.0 \times 10^{14} L_{\odot}$ for the starburst (corrected to the cosmology adopted here). In the case of SMGs, extremely deep X-ray observations strongly suggest that while every SMG probably harbours an AGN, it is the starburst which in almost all cases powers the bulk (70-90 percent) of the FIR luminosity (Alexander et al. 2005), and any AGN contamination would therefore not dramatically affect our conclusions. While optical spectroscopy of J16359 shows no evidence to suggest the presence of strong nuclear activity in this source (Kneib et al. 2004), this is not the case in J02399, which appears to be a type-2 QSO judging from its X-ray emission and optical spectrum properties (Ivison et al. 1998; Vernet & Cimatti 2001). Thus, J02399 could be a rare case where the AGN contribution is substantial. However, given our inability to correct its FIR luminosity for AGN contamination, we estimate the FIR luminosities of both sources simply by fitting a modified black body with a fixed $\beta = 1.5$ to their rest-frame SEDs and integrating it over the wavelength range 40 – 120 μm , see Table 1. This is consistent with the way in which the

FIR-luminosities of the objects observed by Carilli et al. (2005) were calculated. The FIR luminosities for the remaining objects in Table 1 were taken from Carilli et al. (2005) and converted to the cosmology adopted in this paper.

The CO luminosities were taken from the compilation of high- z CO detections in Greve et al. (2005). These are mostly high- J CO detections ($J = 3 - 2$ or $4 - 3$), and in order to derive the CO(1 - 0) line luminosity, we assume optically thick, thermalised CO line ratios, i.e. $(3 - 2)/(1 - 0)$ and $(4 - 3)/(3 - 2) \sim 1$, see Table 1. It should be noted, however, that studies on the ISM in local starburst nuclei yield CO $(3 - 2)/(1 - 0) \sim 0.64$ (Devereux et al. 1994), while first results on ULIRGs yield a CO $(6 - 5)/(4 - 3) \sim 0.6$ ratio but with CO transitions of $J = 4 - 3$ and higher tracing a different H_2 gas phase than the lower three (Papadopoulos, Isaak & van der Werf 2006). These results along with known examples of very low global (high- J)/(low- J) CO ratios in high- z starbursts (e.g. Papadopoulos & Ivison 2002; Greve et al. 2003; Hainline et al. 2006) suggest that we may underestimate the SMG CO(1 - 0) luminosities when we assume line ratios of unity, especially if observed CO $J + 1 \rightarrow J$, $J + 1 \geq 4$ lines are used.

In Figure 2 a) - c) we plot L_{FIR} against L'_{HCN} , L'_{HCN} against L'_{CO} , and L_{FIR} against $L'_{\text{HCN}}/L'_{\text{CO}}$, respectively, for our two sources along with all other existing high- z HCN observations to date. For comparison we have also plotted the sample of local (U)LIRGs (open circles) observed by Gao & Solomon (2004a,b), which defines the local $L_{\text{IR}}-L'_{\text{HCN}}$ relation: $L_{\text{IR}}/L'_{\text{HCN}} = 900 L_{\odot} (\text{K km s}^{-1} \text{pc}^2)^{-1}$. Since we are interested in the correlations with FIR-luminosity, we carefully fitted modified black-body SEDs to the Gao & Solomon sample and derived FIR-luminosities by integrating the SEDs from $40 - 120 \mu\text{m}$. To this end we used all available FIR/submm data in the literature for each source. The resulting local FIR-HCN correlation is given by $\log L_{\text{FIR}} = (0.97 \pm 0.07) \log L'_{\text{HCN}} + (2.9 \pm 0.5)$, and is shown as the solid line in Figure 2 a). The slope of this correlation is consistent with unity, suggesting that the local FIR-HCN correlation is linear (Carilli et al. 2005). In the following we shall use this correlation, along with its $1-\sigma$ limits allowed by the fitting errors (dotted lines in Figure 2 a)), to discuss whether the SMGs and other high- z sources follow the local FIR-HCN correlation. Secondly, motivated by what is seen in local (U)LIRGs, we shall impose a minimum dense gas fraction on the high- z population and from that derive a lower limit on their HCN-luminosity. Finally, we assume the SMGs follow the local FIR-HCN correlation (within $1-\sigma$) and explore what lower limits can be put on their dense gas fraction.

With only four HCN detections to date and little more than a handful of upper limits, including the ones presented here, it is difficult to determine whether the local $L_{\text{FIR}} - L'_{\text{HCN}}$ relation extends to higher redshifts and luminosities. It is interesting to note in Figure 2 a), however, that while the three SMGs with HCN observations (our two sources plus SMM J14011+0252) all are consistent within $1-\sigma$ of the local relation extrapolated to higher

luminosities, 5/7 of the QSOs observed in HCN fall above the $1\text{-}\sigma$ envelope. This may suggest that QSOs have higher FIR luminosities for a fixed HCN luminosity than the SMGs. Although, this is not statistically significant, it is consistent with the expected picture in which the AGN in QSOs contribute a higher fraction to the FIR luminosity than in SMGs. Correcting for the AGN contribution in QSOs would lower them from where they are currently plotted, bringing them more in line with the local $L_{\text{FIR}} - L'_{\text{HCN}}$ correlation.

Alternatively, the data could in principle also be interpreted as a steepening of the slope of the correlation at higher luminosities, meaning that the AGN contribution in both QSOs and SMGs is higher than in local (U)LIRGs – a scenario which would be in line with the suggested increase in AGN dominance with FIR luminosity in local ULIRGs (Veilleux et al. 1999; Tran et al. 2001). Although, X-ray constraints suggest that AGN contribute $\lesssim 30$ percent of to the FIR luminosity of SMGs, they do not allow us to completely rule out the above scenario since it is possible many SMGs harbour obscured, Compton-thick AGN (Alexander et al. 2005). However, the fact that the star formation rates for SMGs derived from reddening-corrected $\text{H}\alpha$ luminosities agree with those derived from their FIR luminosities, suggest that AGN are unlikely to contribute significantly to the FIR.

We see from Figure 2 b) that all the high- z objects lie above the $L'_{\text{HCN}} - L'_{\text{CO}}$ correlation fitted to local galaxies with FIR luminosities less than $10^{11} L_{\odot}$ and with a fixed slope of unity. This is consistent with the steepening of the $L'_{\text{HCN}} - L'_{\text{CO}}$ correlation at higher FIR luminosities seen within the local (U)LIRGs sample itself as reported by Gao & Solomon (2004b). They argued that the dense molecular gas fraction, as gauged by the $L'_{\text{HCN}}/L'_{\text{CO}}$ ratio, is a powerful indicator of starburst dominated systems. Also, locally they found that all galaxies with $L'_{\text{HCN}}/L'_{\text{CO}} \geq 0.06$ have $L_{\text{IR}} \gtrsim 10^{11} L_{\odot}$. In Figure 2 c) we have plotted our estimates of L_{FIR} for the local (U)LIRG sample against their $L'_{\text{HCN}}/L'_{\text{CO}}$ ratios, and find that apart from two sources, the same criterion can be applied to the FIR luminosity, i.e. sources with $L'_{\text{HCN}}/L'_{\text{CO}} \geq 0.06$ have $L_{\text{FIR}} \gtrsim 10^{11} L_{\odot}$. It is also seen that all the high- z sources observed so far – all of which have been very luminous – obey the same criterium. Given their large FIR luminosities, it therefore seems reasonable to assume that the SMGs too have high dense gas fractions, i.e. $L'_{\text{HCN}}/L'_{\text{CO}} \geq 0.06$. In that case, one can put a *lower* limit on their HCN luminosity and investigate where they would lie in the FIR-HCN diagram. The range of allowed HCN luminosities derived in this way for each SMG (and other high- z objects) is shown as horizontal lines in Figure 2a. It is seen that while J02399 and J16359, and the other high- z objects, could lie above the upper dotted line and still have a high dense gas fraction ($L'_{\text{HCN}}/L'_{\text{CO}} \geq 0.06$), this is not the case for J14011. Thus, if our above assumption is correct, we can conclude that at least one of the SMGs (J14011), and possibly more, is consistent with the local FIR-HCN correlation, and that this SMG should be detectable in HCN if the sensitivity is improved by a factor $\times 2$.

APM08279+5255 has the highest measured dense gas fraction, based on detections, in the high- z sample, even though it falls above the local $L_{\text{FIR}} - L'_{\text{HCN}}$ relation in Figure 2 a). Naively, this would indicate that the ISM in this system is dominated by dense gas, and that star formation contributes substantially to its FIR-luminosity. However, caution should be taken since we have calculated the HCN/CO ratio using the nuclear CO line luminosity of APM08279 (Papadopoulos et al. 2001). Adopting the global CO line luminosity, which includes emission extended on 10-kpc scales (Papadopoulos et al. 2001), i.e. scales comparable to those probed by the HCN observations (FWHM $\simeq 7''$ – Waggoner et al. 2005), results in a HCN/CO ratio almost an order of magnitude lower. Similarly, we see that the upper limits on the dense molecular gas fraction in J02399 and J16359 are rather high, yet both sources lie close to the $L_{\text{FIR}} - L'_{\text{HCN}}$ correlation in Figure 2 a). What would the dense gas fraction of the SMGs be if they were required to lie between the upper $1\text{-}\sigma$ line of the local FIR-HCN correlation and their observed HCN limits (for unchanged FIR luminosities)? The answer is given in Figure 2 c), where the permitted range in HCN/CO luminosity ratios are marked as horizontal lines. It is seen that J14011 has a dense gas fraction well within the range of most ULIRGs, and could have $L'_{\text{HCN}}/L'_{\text{CO}} \lesssim 0.06$ and still be consistent with the FIR-HCN correlation. For the other two SMGs we see that even in the most conservative case, where the SMGs are just barely consistent with the $1\text{-}\sigma$ line, they would still have some of the highest dense molecular gas fractions observed, comparable to the most extreme starburst dominated ULIRGs seen locally. Thus we conclude that if the SMGs do in fact follow the FIR-HCN correlation (or are within $1\text{-}\sigma$ of it), then J02399 and J16359 are likely to have higher dense gas fractions than J14011. Note, however, that if an AGN contributes significantly to the FIR luminosity, the above argument would yield a higher HCN luminosity, and thus higher HCN/CO ratios than its true value, but we emphasize that the energy output at FIR/submm wavelengths from AGN in SMGs is found to be negligible compared to the starburst (Alexander et al. 2005).

5. Summary

With this study we have increased the number of submm-selected galaxies with HCN(1–0) observations from 1 to 3, although the upper limit on the HCN luminosity of one of our sources (J16359) is not a very sensitive one. The upper limits on the HCN(1 – 0) line luminosity of these three SMGs are consistent with the $L_{\text{FIR}} - L'_{\text{HCN}}$ relation observed in the local Universe (Gao & Solomon 2004a,b). In order to test whether a typical SMG with a FIR-luminosity of $L_{\text{FIR}} \sim 10^{12.5} L_{\odot}$ is inconsistent with the local relation, we need to be sensitive to HCN luminosities of $L'_{\text{HCN}} \lesssim 10^{10} \text{ K km s}^{-1} \text{ pc}^2$. Thus, we appear to be close (less than a factor of two) in sensitivity to that needed from Figure 2 in order to detect HCN

in SMGs. We conclude that until deeper observations come along there is no evidence to suggest that SMGs have higher star formation efficiencies per unit dense gas mass than local (U)LIRGs or indeed Galactic GMCs (Wu et al. 2005).

We thank the referee for useful comments which helped improve the paper substantially. We are grateful to NRAO for financial and scientific support, and in particular to the telescope operators at Green Bank for their expertise. We thank Ron Maddalena and Toney Minter for their help in reducing the data and for providing the opacity values used. LJH was supported by the GBT graduate student funding program. AWB acknowledges support from the Alfred P. Sloan Foundation and the Research Corporation. IRS acknowledges support from the Royal Society.

REFERENCES

- Alexander, D. M., Bauer, F. E., Chapman, S. C., Smail, I., Blain, A. W., Brandt, W. N., Ivison, R. J. 2005, *ApJ*, 632, 736.
- Barvainis, R., Maloney, P., Antonucci, R., Alloin, D. 1997, *ApJ*, 484, 695.
- Barvainis, R., Alloin D., Bremer, M. 2002, *A&A*, 385, 399.
- Beelen, A. et al. 2004, *A&A*, 423, 441.
- Bertoldi, F., et al. 2003, *A&A*, 409, L47.
- Blain, A. W., et al. 2002, *PhR*, 369, 111.
- Carilli, C. L., et al. 2002, *ApJ*, 575, 145.
- Carilli, C. L., et al. 2005, *ApJ*, 618, 586.
- Devereux, N., Taniguchi, Y., Sanders, D. B., Nakai, N., Young, J. S. 1994, *AJ*, 107, 2006.
- De Breuck, C., Downes, D., Neri, R., van Breugel, W., Reuland, M., Omont, A., Ivison, R. 2005, *A&A*, 430, L1.
- Downes, D., Neri, R., Wiklind, T., Wilner, D. J., Shaver, P. A. 1999, *ApJ*, 513, L1.
- Frayser, D. T., Ivison, R. J., Scoville, N. Z., Yun, M., Evans, A. S., Smail, I., Blain, A. W., Kneib, J.-P. 1998, *ApJ*, 506, L7.
- Frayser, D. T., et al. 1999, *ApJ*, 514, L13.

- Gao, Y. & Solomon, P. M. 2004a, *ApJS*, 152, 63.
- Gao, Y. & Solomon, P. M. 2004b, *ApJ*, 606, 271.
- Genzel, R., Baker, A. J., Tacconi, L. J., Lutz, D., Cox, P., Guilloteau, S., Omont, A. 2003, *ApJ*, 584, 633.
- Greve, T. R., Ivison, R. J., Papadopoulos, P. P. 2003, *ApJ*, 599, 839.
- Greve, T. R., et al. 2005, *MNRAS*, 359, 1165.
- Hainline, L. J., Scoville, N. Z., Yun, M. S., Hawkins, D. W., Frayer, D. T., Isaak, K. G., 2004, *ApJ*, 609, 61.
- Hainline, L. J., et al. 2006, *ApJ*, submitted.
- Isaak, K. G., Chandler, C. J., Carilli, C. L. 2004, *MNRAS*, 348, 1035.
- Ivison, R. J., Smail, Ian, Le Borgne, J.-F., Blain, A. W., Kneib, J.-P., Bezecourt, J., Kerr, T. H., Davies, J. K. 1998, *MNRAS*, 298, 583.
- Kneib, J.-P., van der Werf, P., Knudsen, K. K., Smail, Ian, Blain, A. W., Frayer, D., Barnard, V., Ivison, R. 2004, *MNRAS*, 349, 1211.
- Kneib, J.-P., Neri, R., Smail, I., Blain, A. W., Sheth, K., van der Werf, P., Knudsen, K. K. 2005, *A&A*, 434, 819.
- Neri, R., et al. 2003, *ApJ*, 597, L113.
- Papadopoulos, P. P., Röttgering, H. J. A., van der Werf, P. P., Guilloteau, S., Omont, A., van Breugel, W. J. M. & Tilanus, R. P. J. 2000, *ApJ*, 528, 626.
- Papadopoulos, P. P., Ivison, R. J., Carilli, C. L., Lewis, G. 2001, *Nature*, 409, 58.
- Papadopoulos, P. P. & Ivison, R. J. 2002, *ApJ*, 564, L9.
- Papadopoulos, P. P., Isaak, K. G. & van der Werf, P. 2006, *ApJ*, submitted.
- Rowan-Robinson, M. 2000, *MNRAS*, 316, 885.
- Seaquist, E. R., Ivison, R. J., Hall, P. J. 1995, *MNRAS*, 276, 867.
- Sheth, K., Blain, A. W., Kneib J.-P., Frayer, D. T., van der Werf, P., Knudsen, K. K. 2004, *ApJ*, 614, L5.

- Smail, I., Ivison, R. J., Blain, A. W. 1997, *ApJ*, 490, L5.
- Smail, I., Ivison, R. J., Blain, A. W., Kneib, J.-P. 2002, *MNRAS*, 331, 495.
- Solomon, P. M., Downes, D., Radford, S. J. E. 1992, *ApJ*, 387, L55.
- Solomon, P. M., Vanden Bout, P., Carilli, C. L., Guelin, M., 2003, *Nature*, 426, 636.
- Solomon, P. & Vanden Bout, P. 2005, *ARAA*, 43, 677.
- Spergel, D. N., et al. 2003, *ApJS*, 148, 175.
- Tacconi, L., et al. 2006, *ApJ*, 640, 228.
- Tran, Q. D. et al. 2001, *ApJ*, 552, 527.
- Vanden Bout, P. A., Solomon, P. M., Maddalena, R. J. 2004, *ApJ*, 614, L97.
- Veilleux, S., Kim, D.-C., Sanders, D. B. 1999, *ApJ*, 522, 113.
- Vernet, J. & Cimatti, A. 2001, *A&A*, 380, 409.
- Wagg, J., Wilner, D. J., Neri, R., Downes, D., Wiklind, T. 2005, *ApJ*, 634, L13.
- Walter, F., et al. 2003, *Nature*, 424, 406.
- Weiß, A., Downes, D., Henkel, C. 2005, *A&A*, 440, L45.
- Wilner, D. J., Zhao, J.-H., Ho, P. T. P., 1995, *ApJ*, 453, L91.
- Wu, J., Evans, N. J., Gao, Y., Solomon, P. M., Shirley, Y. L., Vanden Bout, P. A. 2005, *ApJ*, 635, L173.

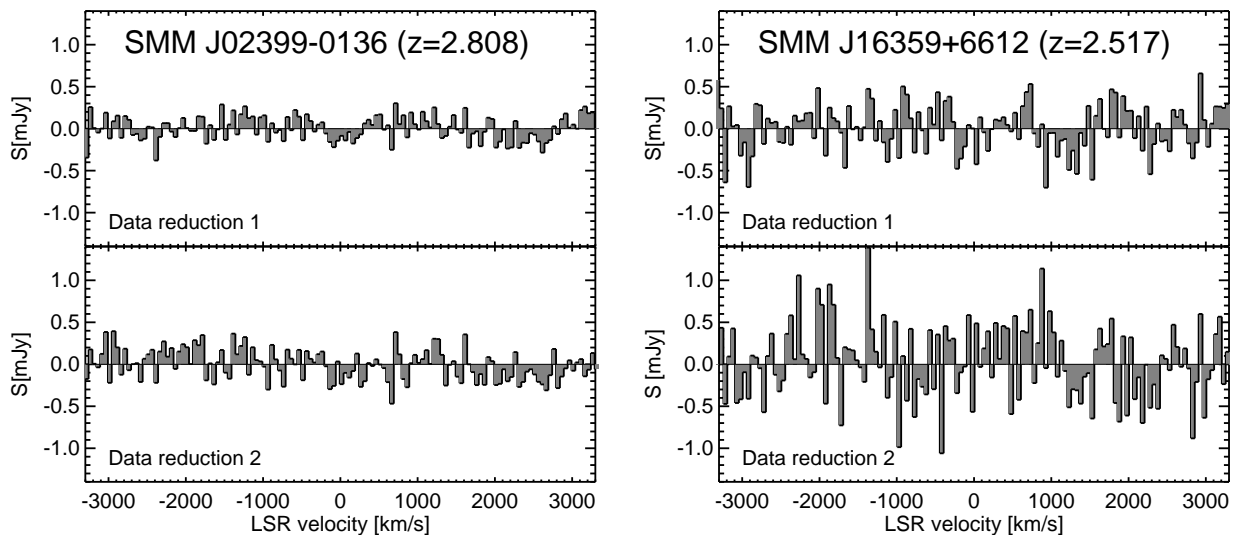


Fig. 1.— HCN($1 - 0$) spectra of J02399 (left) and J16359 (right) produced using the GETNOD routine in GBTIDL (top panels) and our own reduction technique described in §3 (bottom panels). The spectra have been plotted on the same flux- and velocity-scale, making it easier to compare between the different sources and reduction techniques. The LSR velocity-scale is relative to the CO redshift. The spectra have been binned to $\sim 50 \text{ km s}^{-1}$ and the channel-to-channel noise varies between $0.1 - 0.5 \text{ mJy}$.

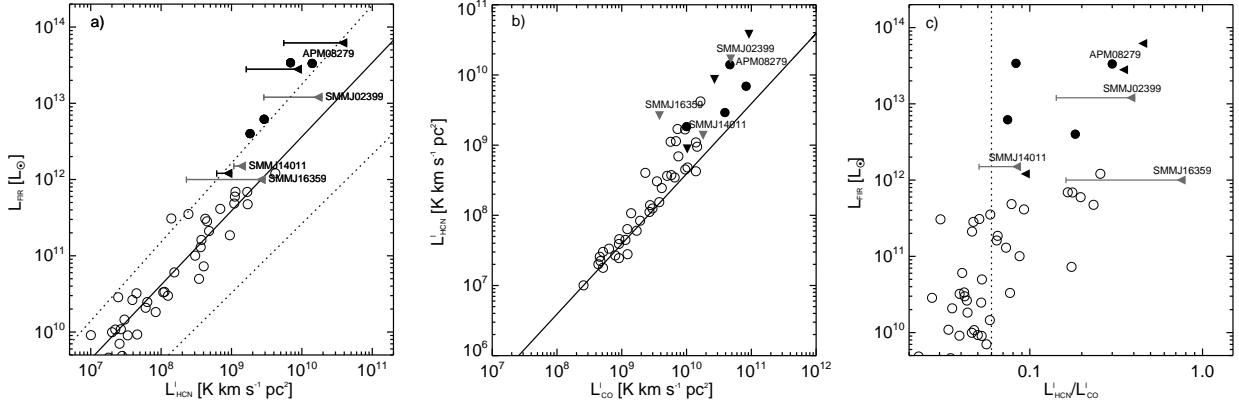


Fig. 2.— Correlations between different combinations of FIR, HCN and CO luminosity for local (U)LIRGs (open circles - Gao & Solomon 2004a,b) and the 10 high- z objects observed in HCN to date (solid circles and triangles). The latter have been corrected for gravitational lensing where appropriate, see Table 1. The three grey triangles denote upper limits of the two SMGs observed as part of this study and SMM J14011+0210 which was observed in HCN by Carilli et al. (2005) using the Very Large Array. The solid line in a) represents the local FIR-HCN correlation derived in this paper: $\log L_{\text{FIR}} = 0.97 \log L'_{\text{HCN}} + 2.8$, while the horizontal extensions to the upper limits mark the L'_{HCN} -range allowed for each source given its observed upper HCN limit and assuming that $L'_{\text{HCN}}/L'_{\text{CO}} \geq 0.06$. The solid line in b) is a fit (with a fixed slope of 1) to normal spiral galaxies in the local Universe. The dotted line in c) marks the $L'_{\text{HCN}}/L'_{\text{CO}}$ limit above which sources in the Gao & Solomon (2004a,b) sample are (U)LIRGs. The range in HCN/CO luminosity ratios for the SMGs, if they were to lie between the upper $1-\sigma$ line of the local $L_{\text{FIR}} - L'_{\text{HCN}}$ correlation, and their observed HCN limits are shown as grey horizontal lines.

Table 1. Observations of HCN at high redshifts to date. The two SMGs studied here are in the upper part of the table. The luminosities have not been corrected for gravitational lensing, but the lensing amplifications (μ) are given in column 9.

Source	Type	z	HCN line	L'_{HCN} $\times 10^{10} \text{ K km s}^{-1} \text{ pc}^2$	CO line	L'_{CO} $\times 10^{10} \text{ K km s}^{-1} \text{ pc}^2$	L_{FIR} $\times 10^{12} L_{\odot}$	μ	Ref.
SMM J02399–0136	SMG	2.808	1–0	≤ 4.9	3–2	12 ± 2	30	2.5	[1],[2],[3]
SMM J16359+6612	SMG	2.517	1–0	≤ 6.7	3–2	8.4 ± 0.4	22	22	[1],[4],[5]
SMM J14011+0252	SMG	2.565	1–0	≤ 0.8	3–2	9.0 ± 0.7	8	5	[6],[7],[8]
SDSS J1148+5251	QSO	6.419	1–0	≤ 1.0	3–2	2.7 ± 0.6	28	1	[6],[9],[10]
BR 1202–0725	QSO	4.693	1–0	≤ 4.4	2–1	9.2 ± 1.0	62	1	[11],[12]
APM 08279+5255	QSO	3.911	5–4	4.2 ± 0.5	1–0	14 ± 3	100	3 ^a	[13],[14],[15]
MG 0751+2716	QSO	3.200	1–0	≤ 1.7	4–3	17 ± 1	20	16.6	[6],[16]
QSO J1409+5628	QSO	2.583	1–0	0.7 ± 0.2	3–2	8.3 ± 0.3	34	1	[6],[17],[18]
H1413+117	QSO	2.558	1–0	3.2 ± 0.6	3–2	43 ± 7	68	11	[19],[18],[19],[20],[21]
	4–3	8.6 ± 1.6		[22]
IRAS F10214+4724	QSO	2.286	1–0	2.2 ± 0.4	3–2	12 ± 3	48	13	[23],[24]

References. — [1] This work; [2] Frayer et al. (1998); [3] Genzel et al. (2003); [4] Sheth et al. (2004); [5] Kneib et al. (2004); [6] Carilli et al. (2005); [7] Frayer et al. (1999); [8] Downes & Solomon (2003); [9] Bertoldi et al. (2003); [10] Walter et al. (2003); [11] Isaak et al. (2004); [12] Carilli et al. (2002); [13] Wagg et al. (2005); [14] Papadopoulos et al. (2001); [15] Lewis et al. (2002); [16] Barvainis et al. (2002); [17] Beelen et al. (2004); [18] Hainline et al. (2004); [19] Solomon et al. (2003); [20] Weiß et al. (2003); [21] Wilner et al. (1995); [22] Barvainis et al. (1997); [23] Vanden Bout et al. (2004); [24] Solomon et al. (1992).

^aWe adopt the lensing amplification derived from high-resolution CO maps by Lewis et al. (2002). Note, however, the amplification factor may be as high as $\mu \sim 7 - 20$ (Downes et al. 1999)